



The UBC27–AIRP3 ubiquitination complex modulates ABA signaling by promoting the degradation of ABI1 in Arabidopsis

Wenbo Pan^{a,b}, Baoying Lin^{a,b}, Xiaoyuan Yang^a, Lijing Liu^c, Ran Xia^a, Jigang Li^d, Yaorong Wu^{a,1}, and Qi Xie^{a,b,1}

^aState Key Laboratory of Plant Genomics, Institute of Genetics and Developmental Biology, The Innovative Academy of Seed Design, Chinese Academy of Sciences, 100101 Beijing, China; ^bCollege of Advanced Agricultural Sciences, University of Chinese Academy of Sciences, 100049 Beijing, China; ^cSchool of Life Sciences, Shandong University, 266237 Qingdao, Shandong, China; and ^dState Key Laboratory of Plant Physiology and Biochemistry, College of Life Sciences, China Agricultural University, 100193 Beijing, China

Edited by Julian I. Schroeder, University of California San Diego, La Jolla, CA, and approved September 15, 2020 (received for review April 22, 2020)

Abscisic acid (ABA) is the key phytohormone in plant drought tolerance and stress adaptation. The clade A protein phosphatase 2Cs (PP2Cs) like ABI1 (ABA-INSENSITIVE 1) work as coreceptors of ABA and regulate multiple ABA responses. Ubiquitination of ABI1 has been proven to play important regulatory roles in ABA signaling. However, the specific ubiquitin conjugating enzyme (E2) involved is unknown. Here, we report that UBC27 is an active E2 that positively regulates ABA signaling and drought tolerance. UBC27 forms the E2–E3 pair with the drought regulator RING E3 ligase AIRP3. Both UBC27 and AIRP3 interact with ABI1 and affect the ubiquitination and degradation of ABI1. ABA activates the expression of UBC27, inhibits the proteasome degradation of UBC27, and enhances the interaction between UBC27 and ABI1 to increase its activity. These findings uncover a regulatory mechanism in ABA signaling and drought response and provide a further understanding of the plant ubiquitination system and ABA signaling pathway.

ubiquitin conjugating enzyme | ABA | ABI1 | ubiquitination | drought response

Drought stress is one of the major limiting factors for crop production worldwide (1). Under drought conditions, a series of stress responsive signal transduction networks are activated to balance growth and stress resistance (1–4), of which the most important is the abscisic acid (ABA) signaling pathway. Under normal conditions, ABA signaling is inhibited by the interaction between clade A protein phosphatase 2Cs (PP2Cs) such as ABI1 and ABI2 and sucrose non-fermenting-1 (SNF1)-related protein kinases (SnRK2s) (5–7). In response to stress, ABA binds its receptors PYRABACTIN RESISTANCE1 (PYR1)/PYR1-LIKE (PYL)/REGULATORY COMPONENTS OF ABA RECEPTORS (RCAR) and mediates their binding to PP2Cs, suppressing the phosphatase activity. This leads to the immediate release of SnRK2s, which induces stomatal closure and downstream gene expression by the phosphorylation of S-type anion channels and some transcription factors (8–10). Thus, the activation of the ABA signaling pathway is regulated by the status of PP2Cs.

Several studies have suggested that posttranslational modifications (PTM) like ubiquitination play a vital role in ABA signaling regulation (11, 12). In ubiquitination, the small molecule ubiquitin (Ub) is attached to target proteins, which modifies their stability, subcellular localization, and activity (13). Ubiquitination involves three main steps: Ub is first activated by the ubiquitin activation enzyme E1, which requires ATP for energy; second, Ub is transferred to the active cysteine residue of ubiquitin-conjugating enzymes E2 through thioester linkage; third, E3 ubiquitin ligase binds E2, then recognizes and ubiquitinates specific substrates. Numerous E3 ligases are involved in plant drought tolerance and ABA signaling (12, 14–16). Ubiquitination of several PP2C members promotes their degradation, thus is important for their activities. For example, the U-box type

E3 ligases PUB12/13 interact with ABI1 coupled to ABA-bound PYR/PYL/RCAR receptors to promote the degradation of ABI1, resulting in the positive regulation of ABA signaling (17). The RING-type E3 ligases RGLG1/5 promote the ubiquitination and degradation of several PP2Cs, like ABI2, HAB2, and PP2CA/AHG3 (18). The substrate adaptors BPM3/5 of the multimeric CRL3 E3 ligase interact with and promote the degradation of PP2Cs like PP2CA, ABI1, ABI2, and HAB1 (19).

Arabidopsis encodes 37 ubiquitin E2s, while functions of many E2s are not well known (20, 21). Studies have demonstrated the role of E2s in the determination of E3 substrate specificity and polyubiquitin chain topology (22, 23). In eukaryote, some E2s were reported to directly bind targets to facilitate the ubiquitination (24, 25). In *Arabidopsis*, the E2 PHO2/UBC24 modulates phosphate homeostasis through directly binding and ubiquitination of the phosphate transporter PHO1 under Pi starvation (25). The endoplasmic reticulum (ER)-localized UBC32 is involved in the degradation of misfolded proteins through ER-associated protein degradation (ERAD) under salt stress (26, 27). In addition, UBC32 itself is ubiquitinated by the E3 ligase HRD1 to tune ERAD activity under normal conditions (28). Recently, UBC32, UBC33, and UBC34 were shown to couple with PUB19 to negatively regulate plant drought tolerance (29). The E2-like protein VPS23 regulates ABA signaling by

Significance

The coreceptors of phytohormone ABA, such as ABI1, are the central regulator of plant tolerance to drought and other abiotic stresses. Tight regulation of ABI1 through ubiquitination is vital for ABA signaling and drought tolerance. In this study, we identified a mechanism to reduce ABI1 protein levels by an E2–E3 pair UBC27–AIRP3. UBC27 directly binds ABI1 and cooperates with AIRP3 in the degradation of ABI1 and ABA signaling. ABA further activates the expression of UBC27 and AIRP3, inhibits the degradation of UBC27, and enhances the interaction between UBC27 and ABI1, establishing a positive feedback regulatory loop to control UBC27 activity under stress conditions. Our results identify a layer of ABA-pathway regulation that terminates ABI1 by the ubiquitination complex UBC27–AIRP3.

Author contributions: W.P., B.L., Y.W., and Q.X. designed research; W.P., B.L., L.L., R.X., and Q.X. performed research; W.P., B.L., X.Y., J.L., and Y.W. analyzed data; and W.P., Y.W., and Q.X. wrote the paper.

The authors declare no competing interest.

This article is a PNAS Direct Submission.

Published under the PNAS license.

¹To whom correspondence may be addressed. Email: yrwu@genetics.ac.cn or qxie@genetics.ac.cn.

This article contains supporting information online at <https://www.pnas.org/lookup/suppl/doi:10.1073/pnas.2007366117/-DCSupplemental>.

First published October 19, 2020.

promoting the endosomal degradation of the ABA receptors PYR1 and PYL4 (30). Among all UBCs in *Arabidopsis*, UBC27 is the only E2 that contains a UBA domain at its C terminus (21, 31), but its biological functions remain to be resolved.

Here, we report a key role for UBC27 in ABA signaling and drought tolerance in *Arabidopsis thaliana*. UBC27 interacts with the RING E3 ligase AIRP3 and forms an E2-E3 pair to promote the ubiquitination and degradation of ABI1. These findings uncover a regulatory mechanism of ABA signaling in plants.

Results

UBC27 Modulates ABA Responses. To explore the roles of E2s in ABA signaling, we tested several transfer DNA (T-DNA) insertion mutants in E2 genes and found that disruption of *UBC27* affects ABA-related cotyledon greening in *Arabidopsis*. The tested homozygous *ubc27-1* mutant in Columbia-0 (Col-0, wild-type, WT) ecotype harbors a T-DNA insertion, which abolishes the expression of *UBC27* (SI Appendix, Fig. S1 A–C). The *ubc27-1* plants did not show visible variation with WT plants under standard growth conditions. While in 1/2 MS medium supplied with 0.25 μ M and 0.5 μ M ABA, *ubc27* mutant lines exhibited a faster cotyledon greening rate (Fig. 1 A and B). No significant difference was observed in the radicle emergence during seed germination. The phenotypic difference was further confirmed in another allele of *ubc27* (SI Appendix, Fig. S1 D and E). These results indicate that *UBC27* is a regulator of ABA-mediated inhibition of cotyledon greening.

Due to the important role of ABA in plant drought tolerance (1, 4), thus we tested the function of *UBC27* in drought tolerance. Plants reduce water loss by closing the stomata in an ABA-dependent manner under drought stress. We first tested the

sensitivity of stomata apertures to ABA treatment in detached leaves from WT and *ubc27* mutants, which showed that the stomata apertures from *ubc27* mutants are less sensitive to ABA treatment (Fig. 1 C and D). The time-resolved stomata conductance of WT and *ubc27* mutant plants in response to ABA treatment (32) was conducted, and the result showed that stomata apertures of *ubc27* are less sensitive to ABA treatment (Fig. 1E and SI Appendix, Fig. S2A). Next, we checked the stomata conductance under drought conditions. The detached leaves from *ubc27* mutant plants also exhibited faster water loss rate compared with WT (Fig. 1F). When whole plants were drought-treated in the soil, the water loss is also faster in *ubc27* mutants (Fig. 1G). Consistent with this point, the *ubc27* mutants exhibited lower leaf surface temperature compared with WT under drought treatment (SI Appendix, Fig. S2B). Since stomata density in plant could also affect those drought-related responses, we measured it and found there was no obvious difference in the stomata density in leaves between WT and *ubc27* (SI Appendix, Fig. S2C). Considering the function of *UBC27* in ABA signaling, these data indicate that the reduced drought tolerance of *ubc27* mutant is caused by ABA-mediated stomatal regulation.

UBC27 Is a Stress Responsive Ubiquitin-Conjugating Enzyme. UBC27 is the sole member of the XII subfamily of E2s in *Arabidopsis* (20, 21), which contains an UBC domain at its N terminus for E2 activity and a UBA domain predicted in its C terminus (SI Appendix, Fig. S3A). UBC27 is highly conserved across fungi, animals, and plants, sharing 53% and 50% identity to UBC1 in yeast and Ubc2K in mammals, respectively (SI Appendix, Fig. S3B).

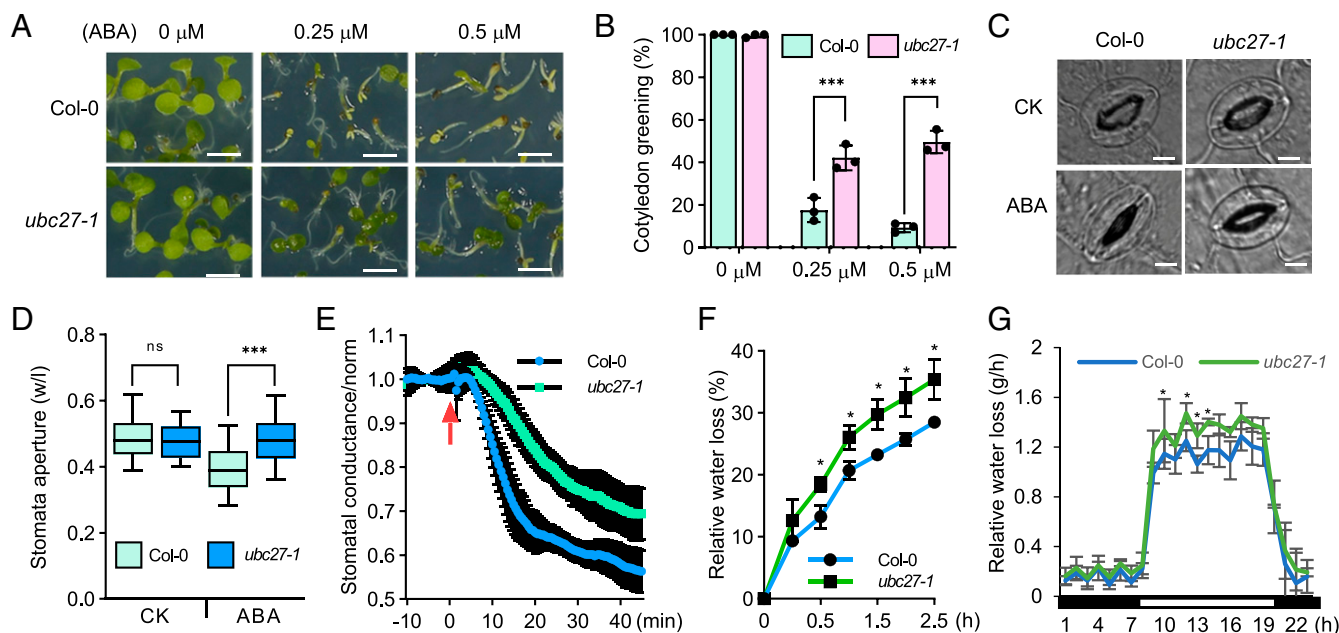


Fig. 1. *UBC27* regulates ABA responses. (A) Photographs of seedlings at 5 dps (days poststratification) on medium containing 0 or 0.25 μ M ABA and 8 dps on medium containing 0.5 μ M ABA. (B) The percentage of seedlings showing green cotyledons in A. Seedlings with expanded cotyledon were considered as green cotyledons. Error bars, SD ($n = 3$). Student's *t* test, *** $P < 0.001$. (C) Photographs of stomata after 2 h of CK or 50 μ M ABA treatment. (D) The ratio of width to length of stomata aperture in C. Data were presented as box and violin with minimum to maximum plots. Student's *t* test, ns, nonsignificant, *** $P < 0.001$. (E) Time-resolved stomatal conductance analysis in response to ABA in detached leaves from WT (Col-0) and *ubc27-1* mutant using a whole-leaf gas exchange analyzer. Data were normalized to the average of the first 10 min of stomatal conductance values recorded. ABA (2 μ M) was added to the transpiration stream (red arrow). $n = 3$ leaves per genotype \pm SD. (F) Water losses of detached leaves from Col-0 and *ubc27-1* plants. Water loss was expressed as the percent of the initial fresh weight (four leaves). Error bars, SD ($n = 3$). Student's *t* test, * $P < 0.05$. (G) Water loss of WT and *ubc27-1* mutant seedlings growing in soil as determined by the weighing of pots over a 24-h period during the drought treatment. The values are means of three replicate pots that were weighed each hour. Black horizontal bars represent the nighttime period, and white horizontal bars represent the daytime period. Error bars, SD ($n = 3$). Student's *t* test, * $P < 0.05$. (Scale bars, A, 2.5 mm; C, 5 μ m.)

To explore the functions of *UBC27* in plants, the expression pattern of *UBC27* was investigated by the β -glucuronidase (*GUS*) reporter assay. Histochemical staining of *GUS* activity revealed that *UBC27* was ubiquitously expressed in seedlings and various tissues, especially in the early germination stages (*SI Appendix, Fig. S4A*). Next, we checked the expression of *UBC27* under ABA and mannitol treatments, a nonabsorbable solute that induces osmotic stress in plants. Transgenic seedlings expressing *GUS* driven by *UBC27* promoter exhibited higher *GUS* activity after treatment (*SI Appendix, Fig. S4B*), and the expression level of *UBC27* was also higher in WT plants after ABA and mannitol treatments (*SI Appendix, Fig. S4C*). These results suggest that *UBC27* is an ABA and osmotic stress responsive gene.

Next, we observed the subcellular localization of *UBC27*. The *UBC27*-green fluorescent protein (*GFP*) fusion protein was localized in cytosol and nuclear subcellular apartments, as it colocalized with a nuclear marker *HY5-RFP* (*SI Appendix, Fig. S4D*) (33). To confirm the E2 activity of *UBC27*, an *in vitro* ubiquitin thioester formation assay (34) was performed. In the presence of FLAG-tagged Ub, E1, and ATP, the *GST-UBC27* protein formed an adduct with Ub through thioester linkage, which disappeared in the presence of the reducing agent DTT (*SI Appendix, Fig. S4E*).

UBC27 Interacts with ABI1

To understand the molecular biological function of *UBC27* in ABA signaling, we attempted to identify its ubiquitination target(s) and other interacting proteins through immunoprecipitation coupled liquid chromatography tandem mass spectrometry (*IP-LC-MS/MS*) analysis. Total proteins from transgenic *Arabidopsis* seedlings overexpressing a *UBC27* HA-tag fusion protein were collected and immunoprecipitated with anti-HA agarose.

Total protein extracted from WT was used as the control sample. The samples were further analyzed with *LC-MS/MS*. *ABI1* was identified among the unique interacting proteins from *UBC27* (*Dataset S1*). The ABA coreceptor *ABI1* negatively regulates ABA signaling by inhibiting the activities of *SnRK2s*, and *ABI1* is known to be ubiquitinated for degradation (17, 19). Thus, *ABI1* is a reasonable candidate for ubiquitination by *UBC27*.

To confirm this hypothesis, we checked the physical interaction between *UBC27* and *ABI1* through a luciferase complementation imaging assay (*LCI*). The *UBC27* and control *UBC8* were fused with the N-terminal fragment of luciferase (*nLUC*), while *ABI1* was fused with the C-terminal fragment of luciferase (*cLUC*). When these proteins were coexpressed in tobacco leaves, we observed a specific luciferase activity signal in the combination of *UBC27* and *ABI1*, but not in the control combinations (*Fig. 2A*). Furthermore, *UBC27-HA* and *myc-ABI1* were coexpressed in tobacco leaves and the coimmunoprecipitation (*Co-IP*) assay was performed. *UBC27-HA* copurified with *myc-ABI1* coupled to anti-myc antibody, but not the *IgG* control (*SI Appendix, Fig. S5A*). We conclude that the E2 enzyme *UBC27* interacts with *ABI1* *in vivo*.

The direct interaction has been detected between mammal *Ube2K*, the homolog of *UBC27*, with its target protein *Huntingtin* (35). We then tested whether the direct interaction occurs between *UBC27* and *ABI1* by biolayer informatory (*BLI*) assay. When proteins bind to a certain surface or another protein, they form a biolayer with increased affinity in thickness, which can be measured by light informatory (36). Incubation of the *Ni-NTA* sensor loaded with *His-UBC27* in solutions containing *MBP-ABI1*, but not the control *MBP* proteins of the same concentrations, resulted in increased biolayer thickness (*Fig. 2B*). The affinity (K_D) of the interaction between *His-UBC27* and *MBP-ABI1*

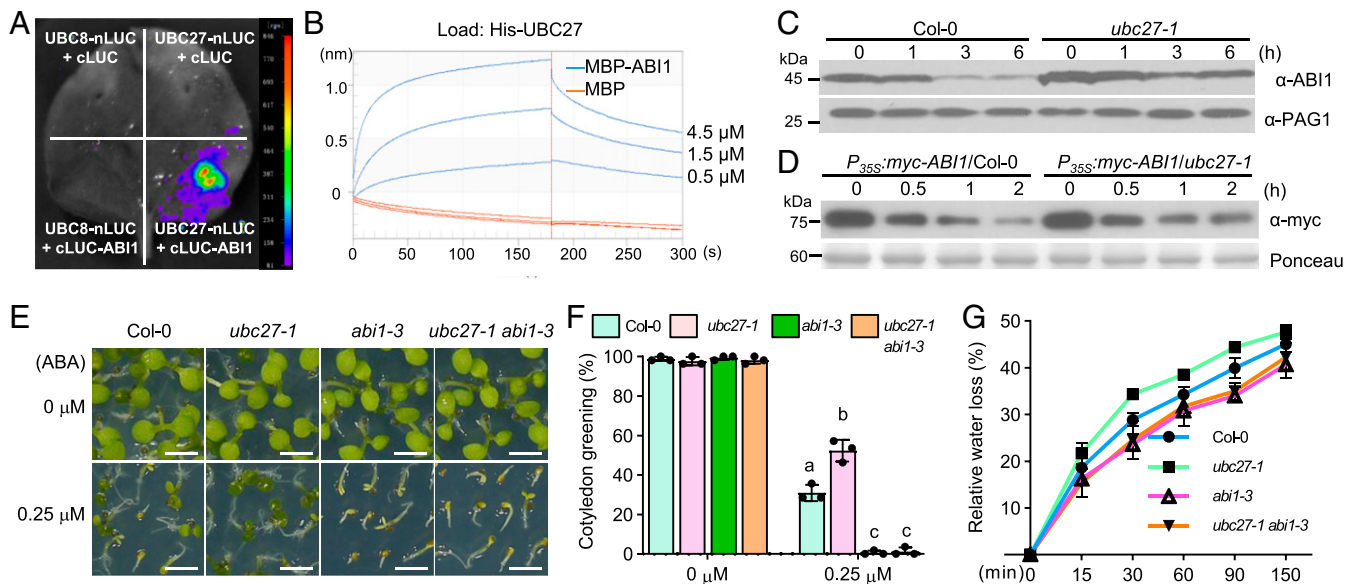


Fig. 2. *UBC27* interacts with and promotes the degradation of *ABI1*. (A) The interaction of *UBC27* with *ABI1* revealed by the *LCI* assay. The indicated construct pairs were coexpressed in tobacco leaves for 3 d before the images were taken. (B) The interaction between *UBC27* and *ABI1* in the *BLI* assay. *Ni-NTA* sensors loaded with *His-UBC27* were exposed to several different concentrations of *MBP-ABI1* or the control protein *MBP* of the same concentrations for 3 min followed by a 2-min dissociation period. The signals indicate the thickness changes of the biolayers. (C) The degradation of *ABI1* in WT and *ubc27-1* mutant seedlings. Ten-day-old *Col-0* and *ubc27-1* seedlings were pretreated with 50 μ M ABA for 2 h to increase the protein level of *ABI1*. The ABA was then washed off, and seedlings were treated with 150 μ M CHX to block protein translation for the indicated times. Anti-PAG1 (20S proteasome α -subunit G1) was used as the loading control. (D) The degradation of *myc-ABI1* in protoplasts from *Col-0* and *ubc27-1*. Lysis of protoplasts from *Col-0* and *ubc27-1* seedlings transfected with equal amount of *myc-ABI1* expressing plasmid constructs were treated with 150 μ M CHX (to block protein translation) and 5 mM ATP for the indicated times. Ponceau staining of *RbcL* was shown as loading control. (E) Photographs of seedlings at 5 dps on 1/2 MS medium containing 0 or 0.25 μ M ABA. (Scale bars, 2.5 mm.) (F) The percentage of seedlings showing green cotyledons in E. Error bars, SD ($n = 3$). Letters above bars indicate significant differences according to two-way ANOVA Tukey's multiple comparisons test ($P < 0.05$). (G) Water loss of detached leaves from indicated seedlings. Water loss was expressed as the percent of the initial fresh weight (four leaves). Error bars, SD ($n = 3$).

was $1,288 \pm 30.24$ nM. The BLI assay suggested the direct interaction between UBC27 and ABI1. We further confirmed this result by in vitro pull-down assay: His-UBC27 could pull down the MBP-ABI1 but not the MBP control itself (*SI Appendix, Fig. S5B*). We further mapped the ABI1 interaction domains in UBC27 based on the defined protein fragments (*SI Appendix, Fig. S5C*). The BLI assay revealed that the interaction affinity between the UBC domain of UBC27 and ABI1 was similar to that of full-length UBC27 and ABI1 (*SI Appendix, Fig. S5D*), and the result was further confirmed by the LCI assay (*SI Appendix, Fig. S5E*). These results suggested that UBC27 directly interacts with ABI1 through its UBC domain.

As UBC27 and ABI1 are involved in ABA signaling, we further tested the effect of ABA treatment on the interaction between UBC27 and ABI1. We observed a stronger interaction when ABA was added in LCI assay, while the protein levels of UBC27 and ABI1 are not significantly changed (*SI Appendix, Fig. S5 F and G*). Similar results were obtained by adding ABA in the Co-IP assay, in which enhanced interaction between UBC27 and ABI1 was detected (*SI Appendix, Fig. S5H*). These results implied a signal-mediated regulation by enhancing the interaction between UBC27 and ABI1 at posttranslational level.

The Ubiquitination and Degradation of ABI1 Are Regulated by UBC27.

The confirmation of the interaction between UBC27 and ABI1 hinted that UBC27 regulates ABI1 stability. First, the specific ABI1 antibody (17) was used to detect the degradation of ABI1 protein in WT and *ubc27-1* plants. After treatment with the translational inhibitor cycloheximide (CHX), ABI1 protein was much more stable in *ubc27-1* mutant plants than that in WT (Fig. 2C and *SI Appendix, Fig. S6A*). Next, a protoplast-based degradation assay was used to analyze the stability of ABI1. The protoplasts from WT and *ubc27-1* mutant plants were transfected with equal amounts of plasmid expressing *myc-ABI1*. Protoplasts were harvested, lysed, and treated with CHX, and ATP (required

for ubiquitination reaction). This experiment also demonstrated that the stability of ABI1 is increased in *ubc27* (Fig. 2D and *SI Appendix, Fig. S6B*). These results indicate that UBC27 is an important regulator of ABI1 degradation.

The Epistatic Relationship Between UBC27 and ABI1. To confirm the functional role of UBC27 in the regulation of ABI1, the *ubc27-1 abi1-3* double mutant was generated and characterized. First, we examined the sensitivity of *ubc27-1 abi1-3* to ABA treatment in cotyledon greening. Knockout of ABI1 rescued the decreased ABA sensitive phenotype of *ubc27-1* (Fig. 2E and F). The genetic relationship between UBC27 and ABI1 in drought tolerance was analyzed too. The *abi1-3* and *ubc27-1 abi1-3* plants exhibited decreased water loss rates, while *ubc27* plants exhibited increased water loss compared with WT in detached leaves (Fig. 2G). The transpiration rate of whole growing plants was analyzed by gravimetric methods under drought treatment. Lower water loss was detected in *ubc27-1 abi1-3* double mutant compared with WT, which was similar to *abi1-3* mutant, but opposite to the *ubc27-1* mutant (*SI Appendix, Fig. S7A*). The leaf surface temperature assay with drought-treated samples also supports the above results (*SI Appendix, Fig. S7B*). Together, these data suggest that the function of UBC27 in ABA signaling and drought tolerance is dependent on ABI1 and that ABI1 is epistatic to UBC27.

The UBC27 Conjugase E2-AIRP3 E3 Ligase Pair. As E2 enzyme UBC27 promotes the degradation of ABI1, we continued to identify the E3 ligase(s) involved in this process. ABI1 is ubiquitinated by U-box type E3 ligases PUB12/13 and CRL3 adaptor BPM3/5 (17, 19). Because single subunit U-box type E3 ligases directly interact with E2s and substrates, the substrate adaptor BTB/POZ proteins of multisubunit CRL3 type E3 ligases don't interact with E2s (20), we investigated the relationship between UBC27 and PUB12/13. We failed to detect the interaction between UBC27 and PUB12/13 in yeast two-hybrid assay where the interaction of UBC27 and Ub was used as the positive control (*SI Appendix, Fig. S8A*). A

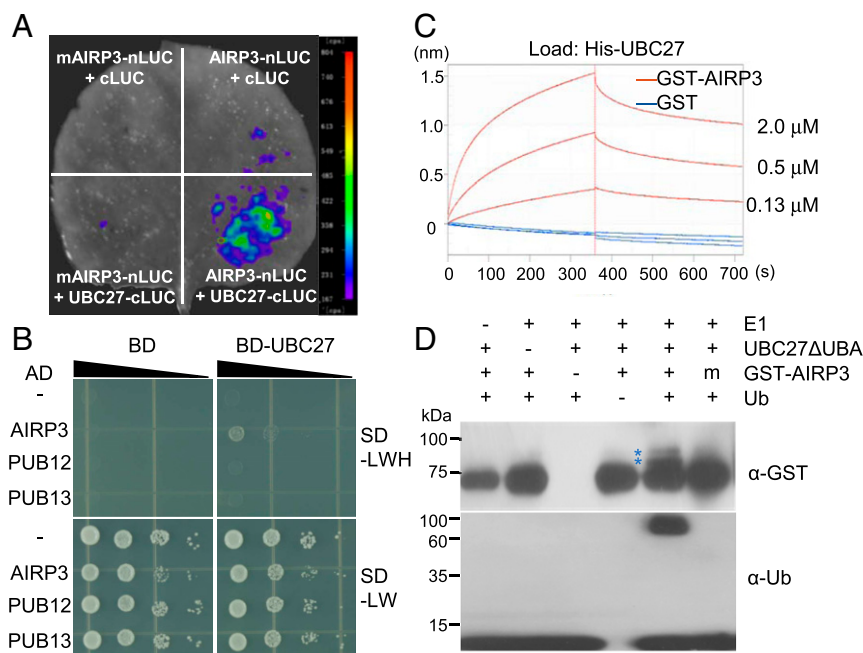


Fig. 3. The E2-E3 pair between UBC27 and AIRP3. (A) The interaction between UBC27 and AIRP3 in LCI assay. The indicated construct pairs were coexpressed in tobacco leaves for 3 d before images were taken. (B) The interaction between UBC27 and AIRP3 in yeast two-hybrid assay. The interaction between AD and BD was used as the negative control. (C) The interaction between UBC27 and AIRP3 in BLI assay. Ni-NTA sensors loaded with His-UBC27 were exposed to several different concentrations of GST-AIRP3 analyte for 6 min followed by a 6-min disassociation period. The GST tag proteins of the same concentrations were used as the negative control. (D) The autoubiquitination activity of AIRP3 in the presence of E1, UBC27 deleted with UBA domain (UBC27 Δ UBA) and Ub. m, function mutated mAIRP3. The ubiquitinated GST-AIRP3 was marked by asterisks and detected with GST and Ub antibodies.

similar result was obtained by LCI assay to test for a potential interaction between UBC27 and PUB12/13 in tobacco leaves (*SI Appendix, Fig. S8B*), indicating that PUB12/13 are not the E3 partners of UBC27 in ABI1 ubiquitination.

Meanwhile, another RING-type E3 ligase, AIRP3, was identified as one of the interacting proteins of UBC27 (*Dataset S1*). AIRP3 is known to positively regulate ABA signaling; the *airp3* mutant exhibits impaired ABA-mediated seed germination inhibition and stomata closure (37), similar to the phenotype of *ubc27*. Therefore, the interaction between UBC27 and AIRP3 was analyzed by LCI assay. When coexpressed, AIRP3-nLUC and UBC27-cLUC exhibited complemented luciferase activity, while mutation in the RING finger, the interaction domain between RING type E3s and E2s, of AIRP3 (AIRP3C319S, mAIRP3) blocked the interaction (*Fig. 3A*). This interaction was also confirmed in yeast two-hybrid assay (*Fig. 3B*). We then investigated the direct interaction of UBC27 and AIRP3 by BLI assay. The GST-AIRP3, but not the control GST, forms new biolayers in Ni-NTA sensors loaded with His-UBC27 (*Fig. 3C*). The affinity (K_D) of the interaction between His-UBC27 and GST-AIRP3 was 187.7 ± 2.25 nM. These results indicate that UBC27 physically interacts with AIRP3.

To test whether UBC27 serves as the E2 for AIRP3, we analyzed the autoubiquitination activity of AIRP3 through in vitro ubiquitination assay. The autoubiquitination activity by full-length UBC27 could hardly be detected in the presence of AIRP3 (*SI Appendix, Fig. S9*). The deletion of the C-terminal

UBA domain promoted the autoubiquitination of AIRP3, while the mutation of RING domain AIRP3 (mAIRP3) blocked the reaction (*Fig. 3D* and *SI Appendix, Fig. S9*). These results suggest that UBC27 forms an E2-E3 pair with AIRP3.

AIRP3 Interacts with ABI1 and Promotes the Degradation of ABI1.

After we discovered that UBC27 promotes the ubiquitination of ABI1 and AIRP3 works as the E3 for UBC27, we next analyzed the involvement of AIRP3 in ABI1 ubiquitination and degradation. The in vivo interaction between AIRP3 and ABI1 was confirmed by LCI assay (*Fig. 4A*). Similar results were obtained from the Co-IP experiment using tobacco leaves expressing both AIRP3-FLAG and myc-ABI1 (*Fig. 4B*). Using a Ni-NTA sensor loaded with His-ABI1, we also detected the increased biolayer thickness when GST-AIRP3 was added, which was not observed in the GST control in the BLI assay (*Fig. 4C*). The affinity (K_D) of His-ABI1 and GST-AIRP3 is 251.4 ± 6.37 nM. These results confirm the physical interaction of AIRP3 and ABI1.

Based on the above findings, we further investigated if AIRP3 regulates the degradation of ABI1. We compared the stability of ABI1 in *airp3* mutants with WT plants using a protoplast-based transient expression assay. Transiently expressed myc-ABI1 was much more stable in protoplasts from *airp3* mutants (*Fig. 4D* and *SI Appendix, Fig. S10A*). We also set up a cell-free degradation assay using recombinant MBP-ABI1 purified from *Escherichia coli*. The degradation of MBP-ABI1 was slower in crude protein extracts from *airp3* mutant plants compared with those from WT

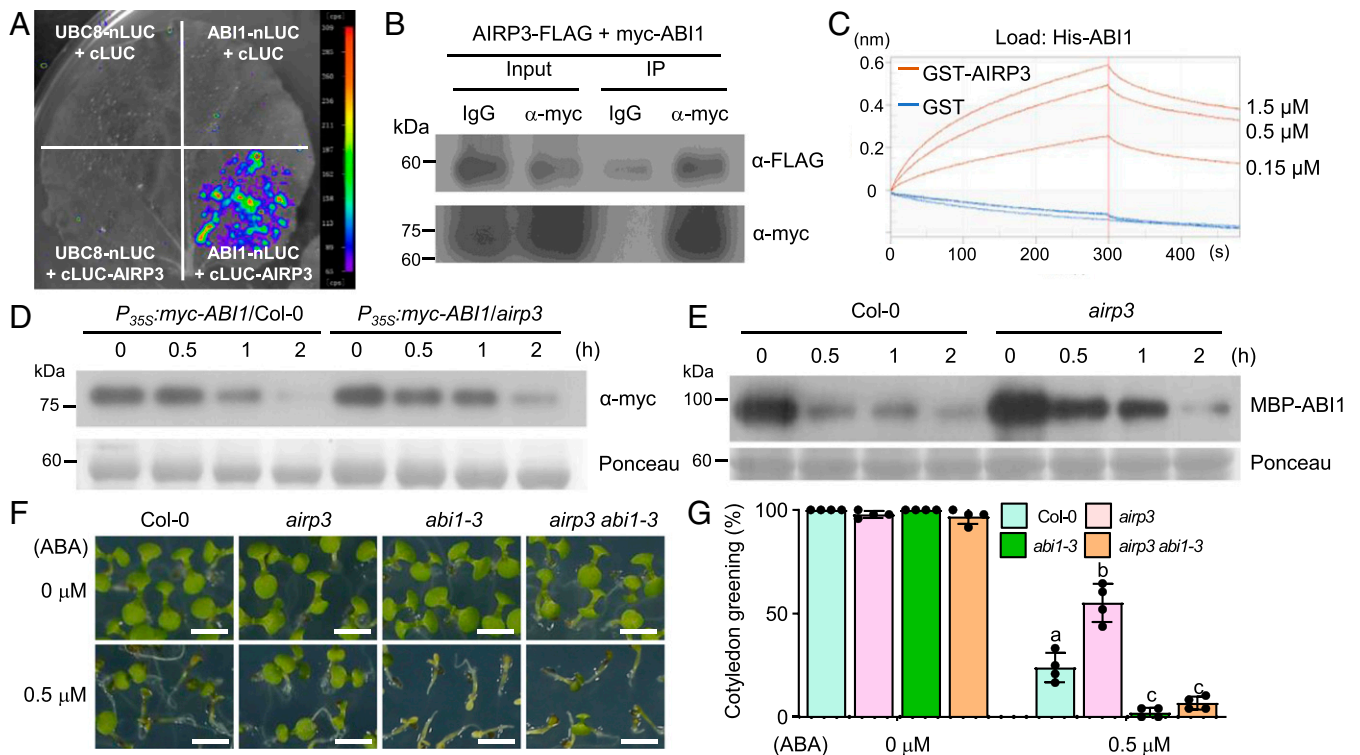


Fig. 4. AIRP3 interacts with ABI1 and promotes the degradation of ABI1. (A) The interaction of AIRP3 with ABI1 in the LCI assay. The indicated construct pairs were coexpressed in tobacco leaves. (B) AIRP3 interacts with ABI1 through the Co-IP assay. Total proteins from tobacco leaves coexpressing AIRP3-FLAG and myc-ABI1 were purified with anti-myc antibody or the IgG control. (C) The interaction between AIRP3 and ABI1 in the BLI assay. Ni-NTA sensors loaded with His-ABI1 were exposed to several different concentrations of GST-AIRP3 for 5 min followed by a 3-min disassociation period. The GST proteins of the same concentrations were used as the negative control. (D) The degradation of myc-ABI1 in protoplast from Col-0 and *airp3*. Lysis of protoplast from Col-0 and *airp3* seedlings transfected with an equal amount of plasmids expressing myc-ABI1 were treated with 150 μ M CHX (to block protein translation) and 5 mM ATP. (E) Cell-free degradation of MBP-ABI1 in protein extracts from Col-0 and *airp3* seedlings. Purified MBP-ABI1 proteins were incubated with extracts of 10-d-old seedlings for the indicated time points. (F) Photographs of seedlings at 5 dps on 1/2 MS medium containing 0 μ M ABA and 8 dps on 1/2 MS medium containing 0.5 μ M ABA. (Scale bars, 2.5 mm.) (G) The percentage of seedlings showing green cotyledons in F was analyzed. Error bars, SD ($n = 4$). Letters above bars indicate significant differences according to two-way ANOVA Tukey's multiple comparisons test ($P < 0.05$).

(Fig. 4E and *SI Appendix*, Fig. S10B). These results demonstrate that the degradation of ABI1 is regulated by AIRP3.

To determine the genetic relationship between *AIRP3* and *ABI1*, we crossed the previously described *airp3* mutant to the *abi1-3* mutant (37). We analyzed ABA-mediated inhibition of cotyledon greening of the *abi1-3 airp3* double mutant. The *abi1-3 airp3* double mutant exhibited enhanced sensitivity to ABA treatment, similar to the *abi1-3* mutant (Fig. 4F and G). This genetic analysis confirms the functional link between *AIRP3* and *ABI1* in ABA signaling.

UBC27 Cooperates with AIRP3 in ABI1 Ubiquitination. Both UBC27 and AIRP3 bind to and promote the degradation of ABI1. We then investigated whether AIRP3 is required for UBC27-mediated ABI1 ubiquitination. As we failed to detect the ubiquitination of bacterial-expressed ABI1 by UBC27 and AIRP3 by the in vitro ubiquitination assay, we set up an in vivo ubiquitination assay by coexpressing UBC27 and AIRP3 with ABI1 in planta. A smeared modification signal for ABI1 was detected when coexpressed with UBC27 and AIRP3. However, this smear was totally abolished upon mutation of the conserved active cysteine of UBC27 (C88S), and was greatly reduced upon mutation of the RING domain of AIRP3 (C319S), both of them greatly reducing their activities (Fig. 5A). Next, we tested the effect of AIRP3 on the interaction of UBC27 and ABI1. The RING-type E3 ligases bind E2 through the RING domain and recruit substrates through their substrate binding domain. If AIRP3 is involved in UBC27-mediated ABI1 ubiquitination, the addition of AIRP3 would facilitate the formation of UBC27–AIRP3–ABI1 complex, while mutation of the RING domain (mAIRP3) would prohibit the interaction between UBC27 and

ABI1. By analyzing the interaction between UBC27 and ABI1 using the LCI assay, we confirmed that their interaction was changed accordingly while the protein levels of UBC27 and ABI1 were not significantly changed with or without functional AIRP3 (Fig. 5B and C). Finally, we generated *AIRP3* overexpression lines in Col-0 and *ubc27-1* mutants. Overexpression of *AIRP3* in Col-0 resulted in enhanced ABA sensitivity in cotyledon greening. Conversely, overexpression of *AIRP3* in *ubc27-1* exhibited reduced ABA sensitivity compared with WT, but was similar to untransformed *ubc27-1* (Fig. 5D and E and *SI Appendix*, Fig. S11). These results all together demonstrated that the E2 ubiquitin conjugase UBC27 cooperates with the RING-type E3 ligase AIRP3 in ABI1 ubiquitination and regulation of ABA signaling.

ABA Inhibits the Degradation of UBC27. The results described above suggest a mechanism for the E2 ubiquitin conjugase UBC27 in ABA signaling. Therefore, we next investigated if UBC27 itself is regulated through ubiquitination. Ubiquitination requires ATP hydrolysis to provide energy for peptide bond formation. We analyzed the stability of UBC27-HA by adding ATP to crude proteins from transgenic *UBC27-HA* overexpression plants in time-course experiments. As shown in Fig. 6A, UBC27 was quite stable without ATP, while ATP induced rapid degradation of UBC27 (Fig. 6A and *SI Appendix*, Fig. S12A). The 26S proteasome inhibitor MG132 significantly repressed the degradation of UBC27 (Fig. 6B and *SI Appendix*, Fig. S12B), indicating that UBC27 was degraded through the 26S proteasome. Finally, we tested whether ABA could, in turn, regulate the stability of UBC27. Interestingly, ABA treatment greatly stabilized UBC27-HA protein in plants (Fig. 6C and *SI Appendix*, Fig. S12C). These

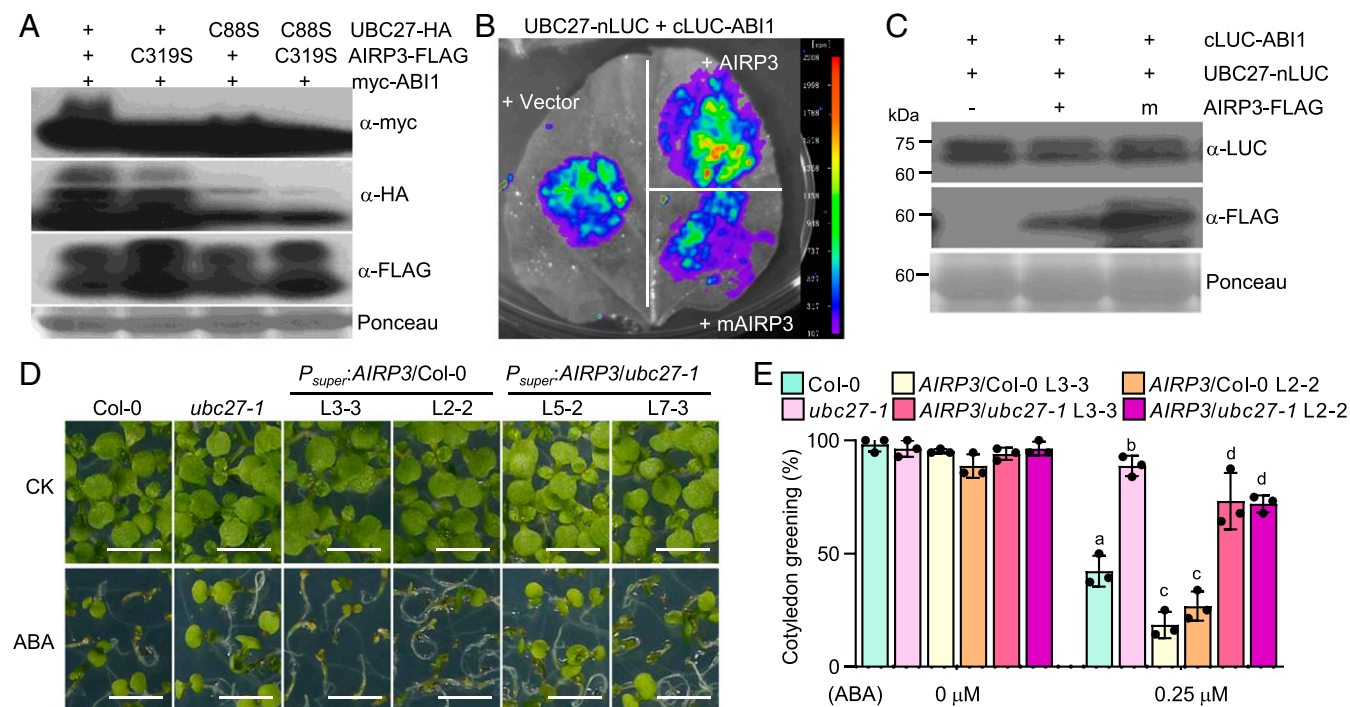


Fig. 5. UBC27 is required for AIRP3-mediated ABI1 ubiquitination and degradation. (A) UBC27 and AIRP3 promote ABI1 ubiquitination. The UBC27, AIRP3, or their functional inactive mutant forms (UBC27C88S and AIRP3C319S, respectively) were coexpressed with ABI1 in tobacco leaves. After treatment with MG132 and ABA for 12 h, total proteins were extracted to check the modification of ABI1. (B) The effect of AIRP3 on the interaction between UBC27 and ABI1. The empty vector, AIRP3-FLAG, and RING domain mutated mAIRP3-FLAG were coexpressed with the same amounts of UBC27-nLUC and cLUC-ABI1. (C) The protein levels of UBC27-nLUC and cLUC-ABI1 in B were detected with anti-LUC antibody (the estimated size of UBC27-nLUC is about 69 kDa and cLUC-ABI1 is about 66 kDa) while the protein levels of AIRP3-FLAG and mAIRP3-FLAG were detected with anti-FLAG antibody. (D) Photographs of seedlings at 5 dps on 1/2 MS medium containing 0 or 0.25 μ M ABA. (Scale bars, 2.5 mm.) (E) The percentage of seedlings showing green cotyledons in D. Error bars, SD ($n = 3$). Letters above bars indicate significant differences according to two-way ANOVA Tukey's multiple comparisons test ($P < 0.05$).

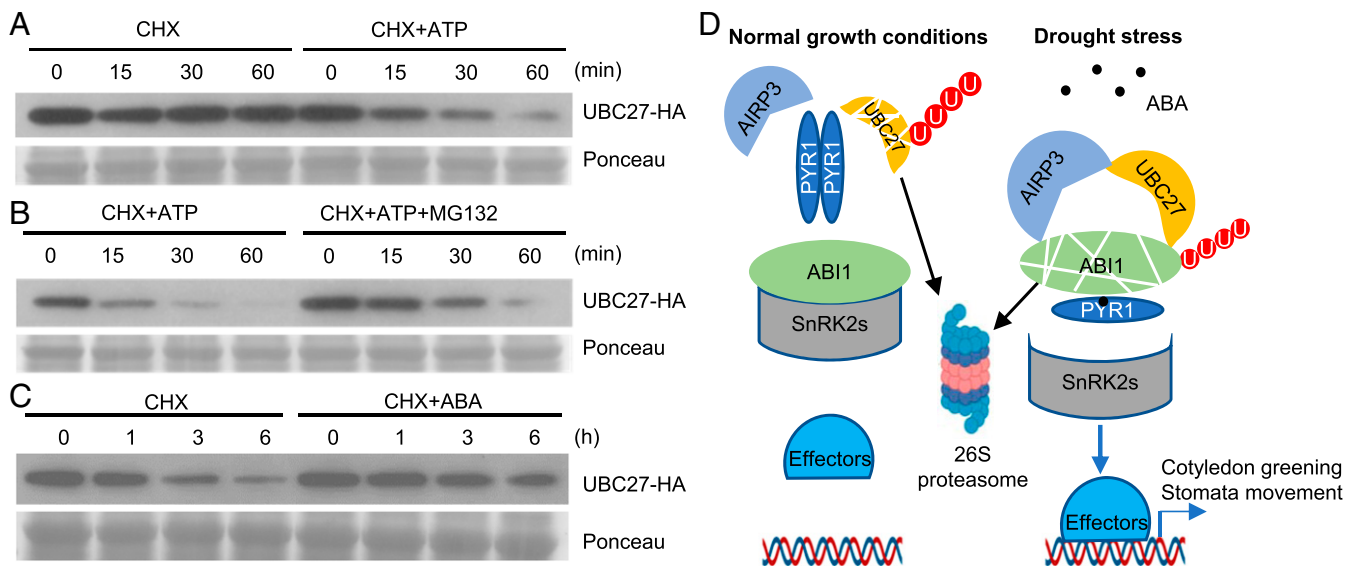


Fig. 6. ABA inhibits the degradation of UBC27 and a working model for UBC27. (A) The effect of ATP on the stability of UBC27. Cell lysis from 10-d-old seedlings overexpressing UBC27-HA was treated with 150 μ M translation inhibitor CHX and ATP. Samples were stopped at indicated time points and checked by immunoblot analysis (anti-HA antibody). Ponceau staining was used as protein loading control. (B) The effect of MG132 on the stability of UBC27. Cell lysis from 10-d-old seedlings overexpressing UBC27-HA was treated with or without 50 μ M MG132. (C) The effect of ABA on the stability of UBC27. Ten-day-old seedlings overexpressing UBC27-HA were treated with CHX and 50 μ M ABA for the indicated time points. Ponceau staining was used as protein loading control. (D) A proposed model for UBC27 in ABA signaling pathway. Under standard growth conditions, the coreceptor ABI1 binds SnRK2s and inhibits the kinase activity of SnRK2s and the downstream ABA responses, under which conditions the UBC27 is ubiquitinated for degradation to inhibit its functions. While plants suffer drought stress, ABA perception by the PYR1/PYLs receptors results in the formation of a PYR1/PYLs-ABA-ABI1 tertiary complex and the release of SnRK2s culminating in the activation of ABA response, which results in the increased expression of *UBC27* and *AIRP3* and facilitates the forming of the E2-E3 pair and the forming of UBC27-ABI1 complex, and the accelerated ubiquitination and degradation of ABI1, resulting in the further activation of ABA responses.

results suggest a feedback regulation mechanism to enhance UBC27 activity by inhibiting the proteasome degradation of UBC27 in ABA signaling.

Discussion

The ABA signaling pathway plays an essential role in regulating plant growth and tolerance to stressful conditions like drought. The coreceptor ABI1 is not only a part of a negative feedback loop within the ABA signaling pathway, but also acts as a hub for hormone cross-talk and is subject to multilevel regulation (17, 19, 38, 39). Our results demonstrate that the ubiquitination of ABI1, mediated by the UBC27-AIRP3 ubiquitination complex, is crucial for ABA responses.

Previous studies have indicated that ubiquitination of ABI1 by E3 ligases PUB12/13 and BPM3/5 is an important regulatory mechanism for regulating ABI1 levels under ABA treatment (17, 19). However, the actual E2 participating in this process was unclear; all reported works used the generic E2, UBC8, which exhibits nearly identical abilities to stimulate ubiquitination of a variety of RING type E3s, for their in vitro ubiquitination assays (20, 21). Here, we found that UBC8 does not interact with ABI1 in vivo (Fig. 24). Although the possibility that UBC8 is also involved in ABI1 ubiquitination cannot be excluded, we showed that the degradation rate of ABI1 is changed in *ubc27* mutant plants (Fig. 2), indicating that UBC27 is vital for ABI1 ubiquitination, illuminating the specific involvement of a novel E2 in ABA signaling.

Several E2s play specific roles in ABA signaling. UBC32/33/34 coupled with PUB19 to negatively regulate ABA-mediated stomatal closure and drought tolerance (29). UBC26 and the RBR type E3 ligase RAF4 form complexes with the ABA receptors PYR1 and PYL4 to negatively regulate ABA signaling (40). UBC27 is a positive regulator of ABA signaling; disruption of *UBC27* affected plant response to ABA treatment in cotyledon

greening and drought tolerance (Fig. 1), which parallels the roles played by *ABI1* in these processes (6).

Commonly, E2 is considered to interact with E3 while E3 specifically recruits substrates (22). However, there are reports that E2 could also directly bind targets. In mammals, E2 protein Apollon directly binds SMAC and caspase-9 to induce apoptosis through ubiquitination-mediated degradation (24). In plants, the E2 conjugase PHO2 directly binds and modulates the stability of the phosphate transporter PHO1 in phosphate homeostasis (25). Here, we discovered that UBC27 could also directly bind ABI1 (Fig. 2 and *SI Appendix*, Fig. S5). These findings suggest the function complexity of ubiquitin conjugase not only providing the E2 activity for ubiquitination but also participating in target recognition.

The regulation of UBC27 itself is also complicated. UBC27 is the sole E2 that contains a UBA domain (20). The mammalian homolog Ube2K is known to catalyze Lys48-linked polyubiquitination with the assistance of the UBA domain (41, 42). UBC27 promotes the degradation of ABI1 through the 26S proteasome, probably through Lys48-linked polyubiquitination (Fig. 2). However, the UBA domain of UBC27 inhibits its E2 activity in vitro, as deletion of the UBA domain enhanced UBC27-mediated AIRP3 autoubiquitination (*SI Appendix*, Fig. S9). We suspect that posttranslational modification(s) might be important for the activation of UBC27 in vivo. The ubiquitination of UBC27 promotes its proteasome degradation and ABA inhibits the degradation of UBC27 in turn (Fig. 6). UBC32 was also ubiquitinated for degradation under standard conditions to tune ERAD activity (28). Tight regulation of E2s through ubiquitination might be a mechanism to balance plant growth and stress tolerance. The expression of *UBC27* is induced by ABA and osmotic stress treatments, and the interaction between UBC27 and ABI1 was enhanced by ABA treatment. These results uncovered multilevel feedback regulation of UBC27 by

ABA at transcriptional and posttranslational levels, which helps us gain further understanding of the complex regulation of the ubiquitination in ABA signaling pathway.

AIRP3 was identified as an interacting protein of UBC27. Previously, AIRP3 was shown to modulate high-salt and drought stress responses through ABA signaling by promoting the degradation of RD21 (37) and to modulate amino acid export by working as the coactivator of GLUTAMINE DUMPER1 (43, 44). Here, we demonstrated that AIRP3 also physically interacts with UBC27 and ABI1 (Figs. 3 and 4). We found that AIRP3 formed an E2-E3 pair with UBC27 and that AIRP3 function depended on UBC27. The degradation of ABI1 was slower in *airp3* mutant plants, and ABI1 is epistatic to AIRP3 (Fig. 4), suggesting a function for AIRP3 in ABA signaling. These results suggest that AIRP3 plays diverse roles by targeting different proteins for degradation. The findings that one E3 can target several different proteins are quite common, such as COP1 targeting HY5, STH, STO, and DELLA (45, 46). Some of the substrates share a common motif, but others do not. Efforts have been made to address this issue (46). However, the detailed recognition mechanism of E3 and substrates needs to be further explored.

Upon to now, three types of E3 ligases (AIRP3, PUB12/13, and CRL3s) have been identified for ABI1 ubiquitination. This means that the ABI1 protein can be regulated by several E3s, which is likely important for the precise modulation of its activity under different conditions or at different subcellular localizations. The ABA receptors, partners of ABI1, are regulated by numbers of different types of E3s. While RSL1 interacts with PYR1 and PYL4 on the plasma membrane (47), AtRAE1, RIFP1, and DDA1, respectively, interact with RCAR1, RCAR3, and PYL8 in the nucleus (48–50). Clade A PP2Cs are regulated by PUB12/13 (17), BPM3/5 (19), RGLG1/5 (18), and AIRP3. RGLG1 is attached to the plasma membrane through myristoylation (51). However, ABA treatment inhibits the myristoylation of RGLG1 by the down-regulation of *N-myristoyltransferase 1* (*NMT1*), thus promoting the nuclear translocation of RGLG1 and the formation of the RGLG1–PP2CA complex (51). A similar mechanism might exist for AIRP3, as AIRP3 is also myristoylated *in vivo* (44). The subcellular location of the AIRP3 and ABI1 interaction and

whether it plays different roles from PUB12/13 and BPM3/5 require further study.

UBC27 and AIRP3 are ubiquitously expressed and induced by ABA treatment (*SI Appendix*, Fig. S4) (37). It has been proven that the ubiquitination and degradation of ABI1 is enhanced by ABA treatment (17, 19). These results show that the increased ubiquitination and degradation of ABI1 are important to regulate the protein levels of ABI1, which result in a feedback regulation to further activate the ABA response. Thus, we propose a mechanism by which UBC27 and AIRP3 modulate ABA signaling and drought tolerance (Fig. 6D). In standard growth conditions, the ABA coreceptor ABI1 binds SnRK2s and inhibits the kinase activity of SnRK2s. UBC27 is unstable and degraded through the 26S proteasome to minimize its activity and keep the ABA signaling in the resting state. Under drought stress conditions, ABA perception by PYR1/PYLs receptors results in the formation of a PYR1/PYLs–ABA–ABI1 tertiary complex and the release of SnRK2s. The E2 conjugase UBC27 and E3 ligase AIRP3 form a ubiquitination complex and promote the degradation of ABI1, resulting in the further activation of ABA responses. ABA in turn stabilizes UBC27 and promotes the formation of UBC27–ABI1 complex. Our model suggests that UBC27–AIRP3-mediated ABI1 ubiquitination and degradation is a key component of plant ABA signaling and drought tolerance.

Materials and Methods

Detailed description of the plant materials and growth conditions, and methods used for protein–protein interaction assays, protein localization, *in vitro* and *in vivo* ubiquitination can be found at *SI Appendix, Materials and Methods*.

Data Availability. All data discussed in the paper are available in the main text and *SI Appendix*.

ACKNOWLEDGMENTS. We thank Dr. Zhizhong Gong and Dr. Lingyao Kong from China Agricultural University for their valuable technical support in this study. We thank Dr. Xiangdong Fu and Dr. Yajun Pan from the Institute of Genetics and Developmental Biology, Chinese Academy of Sciences, for their assistance in thermal imaging and time-resolved stomatal conductance analysis. This work was financially supported by National Key R&D Program of China Grant 2016YFA0500501 and National Natural Science Foundation Grant 31972862 of China.

- J. K. Zhu, Abiotic stress signaling and responses in plants. *Cell* **167**, 313–324 (2016).
- J. K. Zhu, Salt and drought stress signal transduction in plants. *Annu. Rev. Plant Biol.* **53**, 247–273 (2002).
- K. Shinozaki, K. Yamaguchi-Shinozaki, Gene networks involved in drought stress response and tolerance. *J. Exp. Bot.* **58**, 221–227 (2007).
- K. Chen *et al.*, Abscisic acid dynamics, signaling, and functions in plants. *J. Integr. Plant Biol.* **62**, 25–54 (2020).
- Y. Ma *et al.*, Regulators of PP2C phosphatase activity function as abscisic acid sensors. *Science* **324**, 1064–1068 (2009).
- K. Meyer, M. P. Leube, E. Grill, A protein phosphatase 2C involved in ABA signal transduction in *Arabidopsis thaliana*. *Science* **264**, 1452–1455 (1994).
- S. Merlot, F. Gosti, D. Guerrier, A. Vavasseur, J. Giraudat, The ABI1 and ABI2 protein phosphatases 2C act in a negative feedback regulatory loop of the abscisic acid signalling pathway. *Plant J.* **25**, 295–303 (2001).
- T. Umezawa *et al.*, Type 2C protein phosphatases directly regulate abscisic acid-activated protein kinases in *Arabidopsis*. *Proc. Natl. Acad. Sci. U.S.A.* **106**, 17588–17593 (2009).
- S. R. Cutler, P. L. Rodriguez, R. R. Finkelstein, S. R. Abrams, Abscisic acid: Emergence of a core signaling network. *Annu. Rev. Plant Biol.* **61**, 651–679 (2010).
- S. Y. Park *et al.*, Abscisic acid inhibits type 2C protein phosphatases via the PYR/PYL family of START proteins. *Science* **324**, 1068–1071 (2009).
- D. R. Kelley, M. Estelle, Ubiquitin-mediated control of plant hormone signaling. *Plant Physiol.* **160**, 47–55 (2012).
- F. Yu, Y. Wu, Q. Xie, Ubiquitin-proteasome system in ABA signaling: From perception to action. *Mol. Plant* **9**, 21–33 (2016).
- A. Ciechanover, The unravelling of the ubiquitin system. *Nat. Rev. Mol. Cell Biol.* **16**, 322–324 (2015).
- J. A. Sullivan, K. Shirasu, X. W. Deng, The diverse roles of ubiquitin and the 26S proteasome in the life of plants. *Nat. Rev. Genet.* **4**, 948–958 (2003).
- N. Shabek, N. Zheng, Plant ubiquitin ligases as signaling hubs. *Nat. Struct. Mol. Biol.* **21**, 293–296 (2014).
- H. Liu, S. L. Stone, E3 ubiquitin ligases and abscisic acid signaling. *Plant Signal. Behav.* **6**, 344–348 (2011).
- L. Kong *et al.*, Degradation of the ABA co-receptor ABI1 by PUB12/13 U-box E3 ligases. *Nat. Commun.* **6**, 8630 (2015).
- Q. Wu *et al.*, Ubiquitin ligases RGLG1 and RGLG5 regulate abscisic acid signaling by controlling the turnover of phosphatase PP2CA. *Plant Cell* **28**, 2178–2196 (2016).
- J. Julian *et al.*, The MATH-BTB BPM3 and BPM5 subunits of Cullin3-RING E3 ubiquitin ligases target PP2CA and other clade A PP2Cs for degradation. *Proc. Natl. Acad. Sci. U.S.A.* **116**, 15725–15734 (2019).
- J. Callis, The ubiquitination machinery of the ubiquitin system. *Arabidopsis Book* **12**, e0174 (2014).
- E. Kraft *et al.*, Genome analysis and functional characterization of the E2 and RING-type E3 ligase ubiquitination enzymes of *Arabidopsis*. *Plant Physiol.* **139**, 1597–1611 (2005).
- Y. Ye, M. Rape, Building ubiquitin chains: E2 enzymes at work. *Nat. Rev. Mol. Cell Biol.* **10**, 755–764 (2009).
- M. D. Stewart, T. Ritterhoff, R. E. Kleivit, P. S. Brzovic, E2 enzymes: More than just middle men. *Cell Res.* **26**, 423–440 (2016).
- Y. Hao *et al.*, Apollon ubiquitinates SMAC and caspase-9, and has an essential cyto-protection function. *Nat. Cell Biol.* **6**, 849–860 (2004).
- T. Y. Liu *et al.*, PHO2-dependent degradation of PHO1 modulates phosphate homeostasis in *Arabidopsis*. *Plant Cell* **24**, 2168–2183 (2012).
- F. Cui *et al.*, *Arabidopsis* ubiquitin conjugase UBC32 is an ERAD component that functions in brassinosteroid-mediated salt stress tolerance. *Plant Cell* **24**, 233–244 (2012).
- L. Liu *et al.*, The endoplasmic reticulum-associated degradation is necessary for plant salt tolerance. *Cell Res.* **21**, 957–969 (2011).
- Q. Chen *et al.*, HRD1-mediated ERAD tuning of ER-bound E2 is conserved between plants and mammals. *Nat. Plants* **2**, 16094 (2016).

29. M. Y. Ahn *et al.*, Arabidopsis group XIV ubiquitin-conjugating enzymes AtUBC32, AtUBC33, and AtUBC34 play negative roles in drought stress response. *J. Plant Physiol.* **230**, 73–79 (2018).
30. F. Yu *et al.*, ESCRT-I component VPS23A affects ABA signaling by recognizing ABA receptors for endosomal degradation. *Mol. Plant* **9**, 1570–1582 (2016).
31. A. Ramadan *et al.*, Wheat germ-based protein libraries for the functional characterisation of the Arabidopsis E2 ubiquitin conjugating enzymes and the RING-type E3 ubiquitin ligase enzymes. *BMC Plant Biol.* **15**, 275 (2015).
32. P. H. O. Ceciliato *et al.*, Intact leaf gas exchange provides a robust method for measuring the kinetics of stomatal conductance responses to abscisic acid and other small molecules in *Arabidopsis* and grasses. *Plant Methods* **15**, 38 (2019).
33. H. Zhang *et al.*, The RING finger ubiquitin E3 ligase SDIR1 targets SDIR1-INTERACTING PROTEIN1 for degradation to modulate the salt stress response and ABA signaling in *Arabidopsis*. *Plant Cell* **27**, 214–227 (2015).
34. Q. Zhao *et al.*, A plant-specific in vitro ubiquitination analysis system. *Plant J.* **74**, 524–533 (2013).
35. M. A. Kalchman *et al.*, Huntingtin is ubiquitinated and interacts with a specific ubiquitin-conjugating enzyme. *J. Biol. Chem.* **271**, 19385–19394 (1996).
36. J. Concepcion *et al.*, Label-free detection of biomolecular interactions using Biolayer interferometry for kinetic characterization. *Comb. Chem. High Throughput Screen.* **12**, 791–800 (2009).
37. J. H. Kim, W. T. Kim, The Arabidopsis RING E3 ubiquitin ligase AtAIRP3/LOG2 participates in positive regulation of high-salt and drought stress responses. *Plant Physiol.* **162**, 1733–1749 (2013).
38. M. Tajdel, F. Mitula, A. Ludwikow, Regulation of Arabidopsis MAPKKK18 by ABI1 and SnRK2, components of the ABA signaling pathway. *Plant Signal. Behav.* **11**, e1139277 (2016).
39. Y. Li, Y. Li, Y. Liu, Y. Wu, Q. Xie, The sHSP22 heat shock protein requires the ABI1 protein phosphatase to modulate polar auxin transport and downstream responses. *Plant Physiol.* **176**, 2406–2425 (2018).
40. M. A. Fernandez *et al.*, RBR-type E3 ligases and the Ub-conjugating enzyme UBC26 regulate ABA receptor levels and signaling. *Plant Physiol.* **182**, 1723–1742 (2020).
41. J. G. Lee *et al.*, Crystal structure of the Ube2K/E2-25K and K48-linked di-ubiquitin complex provides structural insight into the mechanism of K48-specific ubiquitin chain synthesis. *Biochem. Biophys. Res. Commun.* **506**, 102–107 (2018).
42. R. C. Wilson, S. P. Edmondson, J. W. Flatt, K. Helms, P. D. Twigg, The E2-25K ubiquitin-associated (UBA) domain aids in polyubiquitin chain synthesis and linkage specificity. *Biochem. Biophys. Res. Commun.* **405**, 662–666 (2011).
43. D. Guerra *et al.*, Control of amino acid homeostasis by a ubiquitin ligase-coactivator protein complex. *J. Biol. Chem.* **292**, 3827–3840 (2017).
44. R. Pratelli *et al.*, The ubiquitin E3 ligase LOSS OF GDU2 is required for GLUTAMINE DUMPER1-induced amino acid secretion in *Arabidopsis*. *Plant Physiol.* **158**, 1628–1642 (2012).
45. N. Blanco-Touriñán *et al.*, COP1 destabilizes DELLA proteins in *Arabidopsis*. *Proc. Natl. Acad. Sci. U.S.A.* **117**, 13792–13799 (2020).
46. M. Holm, C. S. Hardtke, R. Gaudet, X. W. Deng, Identification of a structural motif that confers specific interaction with the WD40 repeat domain of Arabidopsis COP1. *EMBO J.* **20**, 118–127 (2001).
47. E. Bueso *et al.*, The single-subunit RING-type E3 ubiquitin ligase RSL1 targets PYL4 and PYR1 ABA receptors in plasma membrane to modulate abscisic acid signaling. *Plant J.* **80**, 1057–1071 (2014).
48. D. Li *et al.*, AtRAE1 is involved in degradation of ABA receptor RCAR1 and negatively regulates ABA signalling in *Arabidopsis*. *Plant Cell Environ.* **41**, 231–244 (2018).
49. Y. Li *et al.*, The Arabidopsis F-box E3 ligase RIFP1 plays a negative role in abscisic acid signalling by facilitating ABA receptor RCAR3 degradation. *Plant Cell Environ.* **39**, 571–582 (2016).
50. M. L. Irigoyen *et al.*, Targeted degradation of abscisic acid receptors is mediated by the ubiquitin ligase substrate adaptor DDA1 in *Arabidopsis*. *Plant Cell* **26**, 712–728 (2014).
51. B. Belda-Palazon *et al.*, ABA inhibits myristoylation and induces shuttling of the RGLG1 E3 ligase to promote nuclear degradation of PP2CA. *Plant J.* **98**, 813–825 (2019).